THE JOURNAL OF PHYSICAL CHEMISTRY B

Article

pubs.acs.org/JPCB

MS-CASPT2 Study of Hole Transfer in Guanine–Indole Complexes Using the Generalized Mulliken–Hush Method: Effective Two-State Treatment

C. Butchosa,[†] S. Simon,[†] L. Blancafort,*[,†] and A. Voityuk*[,†,‡]

[†]Institut de Química Computacional, Departament de Química, Universitat de Girona, Campus de Montilivi, Girona, 17071 Spain

[‡]Institució Catalana de Recerca i Estudis Avançats (ICREA), Barcelona, 08010 Spain

Supporting Information

ABSTRACT: Because hole transfer from nucleobases to amino acid residues in DNA–protein complexes can prevent oxidative damage of DNA in living cells, computational modeling of the process is of high interest. We performed MS-CASPT2 calculations of several model structures of π-stacked guanine and indole and derived electron-transfer (ET) parameters for these systems using the generalized Mulliken–Hush (GMH) method. We show that the two-state model commonly applied to treat thermal ET between adjacent donor and acceptor is of limited use for the considered systems because of the small gap between the ground and first excited states in the indole radical cation. The ET parameters obtained within the two-state GMH scheme can deviate significantly from the corresponding matrix elements of the two-state effective Hamiltonian based on the GMH treatment of three adiabatic states. The computed values of diabatic energies and electronic couplings provide benchmarks to assess the performance of less sophisticated computational methods.

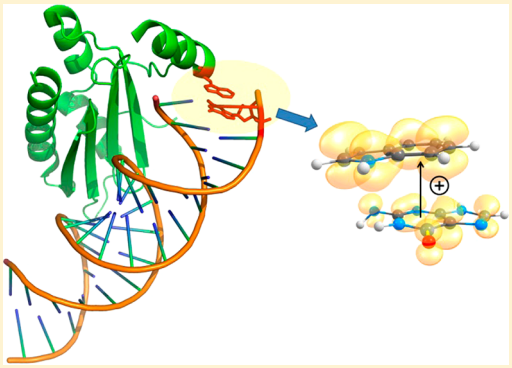

INTRODUCTION

During the past three decades, hole transfer (migration of radical cation states) through DNA and its artificial analogues has been an area of extensive experimental and theoretical studies.[1−5] Attention to this field is motivated by the role played by hole transfer (HT) in several biological processes such as damage and repair of DNA and mediation of signaling in living cells.[6] In particular, special proteins called photolyases can repair damaged DNA in living cells.[7] The underlying mechanism has been analyzed by computational studies (see recent articles[8,9] and references therein). Also, migration of a hole from DNA to a neighboring cofactor or an amino acid residue of the protein environment can protect genomic DNA from the oxidative damage. This implies that HT is faster than irreversible reactions of the radical cation state of a nucleobase with water, oxygen, and other species leading to the formation of DNA lesions.[6,10]

The formation of radical cation states in biomolecules is controlled by their oxidation potential. Among natural nucleobases, guanine has the lowest ionization energy and acts as a hole trap in DNA. In proteins, the best hole acceptor is the amino acid tryptophan (Trp), the indole group (Ind) of which can effectively trap an electron hole. In particular, it was experimentally found that the guanine radical cation is able to oxidize tryptophan residues.[11,12] Whereas hole migration through DNA π stacks is well-documented,[1−5] much is still unknown about HT in DNA–protein complexes. Only a few computational studies of HT between nucleobases and amino acid residues have been reported.[13,14] Density functional theory (DFT) calculations of indole complexes with guanine (G) and adenine (A) showed that the HT process can occur not only in π-stacked but also in T-shaped structures, where the aromatic rings of Ind and G or A are perpendicular to each other. It was also found that the driving force and electronic coupling of the HT depend significantly on the mutual orientation of the donor and acceptor sites.[15−17]

Distinct from radical cations G^+ and A^+, Ind^+ has a small energy gap between the ground and first excited states, as shown in Figure 1. Experimental values of the vertical ionization energies were obtained from refs 18 and 19. The excited state in G^+ lies 1.6 eV higher than the ground state, whereas the energy gap in Ind^+ is only ∼0.5 eV. This means that the excited state of Ind^+ can affect the thermal HT process $G^+ + Ind \rightarrow G + Ind^+$. To take this effect into account, a three-state scheme rather than the commonly used two-state scheme must be applied to derive the site energies and coupling for thermal HT between G^+ and Ind. Moreover, because the HT parameters depend on the mutual positions of the redox centers, the contribution of the Ind^+ excited state is expected to be sensitive to the orientations of the G and Ind molecules.

Received: April 17, 2012
Revised: June 5, 2012
Published: June 14, 2012

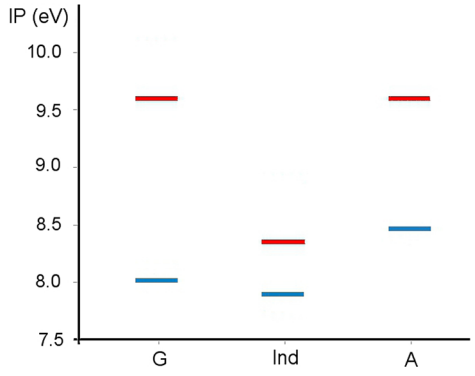

Figure 1. First and second ionization energies (in blue and red, respectively) of guanine (G), indole (Ind), and adenine (A).

Therefore, several configurations of the system must be examined.

In this article, we report high-level ab initio calculations (at the MS-CASPT2 level) of several π-stacked structures of G and Ind and the HT parameters derived therefrom using the generalized Mulliken–Hush (GMH) method.[20] The need to include a third state in GMH calculations for organic donor–acceptor systems was previously considered by Cave and co-workers,[21] who compared the couplings obtained with two-state and three-state treatments and proposed an effective two-state expression for the couplings. Here, we consider also the effect of the third state on the diabatic energies and the driving force of HT. A simple and intuitive rule, based on the dipole moments of the diabatic states, is introduced to estimate whether the three-state treatment is necessary. As shown herein, the data obtained with the two- and three-state GMH treatments can differ significantly. This indicates the limited use of the two-state scheme. Our MS-CASPT2 results can also be used to assess the performance of less sophisticated computational methods in the treatment of HT in DNA–protein complexes. Similarly, the MS-CASPT2 data obtained for HT in stacks of nucleobases[22] have been widely employed to check the accuracy of DFT[23−26] and semiempirical methods.[27]

COMPUTATIONAL DETAILS

Electronic Structure Calculations. The CASSCF (complete-active-space self-consistent-field), CASPT2 (complete-active-space second-order perturbation theory), and MS-CASPT2 (multistate formulation of CASPT2 that accounts for the nonorthogonality of the CASPT2 wave function)[28] calculations were carried out for several π-stacked $(G–Ind)^{\bullet+}$ structures using the ANO-S basis set and an active space of 11 electrons in 12 orbitals (11,12). This active space comprises six π orbitals on each molecule. A real level shift parameter of 0.2 was used.[29] The energies were obtained from a single-point calculation, using state-averaged orbitals over five states, with equal weights for each state. Five states were computed to check whether additional states had to be included in the multistate electronic coupling calculation. The energy gap between the third and fourth states was always larger than 1 eV (see Table SI1 in the Supporting Information), and therefore, the fourth and fifth states were not included in the GMH approach. The dipole moment of each state and the transition dipole moments were derived from the perturbationally modified CAS configuration interaction (PM-CASCI) wave function that was obtained from the MS-CASPT2 calculation. For comparison, we include in the Supporting Information the electron-transfer (ET) parameters based on the CASSCF energies and dipole moments (Table SI3, Supporting Information). The parameters differ by up to an order of magnitude, which shows that the MS-CASPT2 level is necessary for an accurate treatment. The calculations were carried out with MOLCAS 7.2.[30]

Geometries. A set of six $(G–Ind)^{\bullet+}$ stacked conformations with a parallel arrangement of the subunits was generated (see Figure 2). These structures were used in our previous DFT

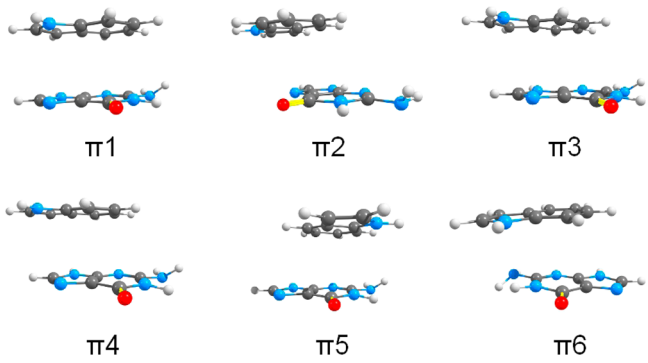

Figure 2. Structures of guanine–indole complexes.

study on electronic coupling in $(G–Ind)^{\bullet+}$ systems,[16] and we keep the nomenclature used there. In all conformations, the distance between the planes of the molecules (rise parameter) was set to 3.38 Å. The reference structure is π1 with optimal stacking of the aromatic rings. Structure π2 was obtained from π1 displacing the indole unit by 2.0 Å along the shift direction, whereas structures π3 and π4 were obtained by displacements of −1.7 and 2.7 Å, respectively, along the slide direction. Structure π5 was generated by rotating the indole unit of π1 by 110°, and structure π6 was obtained by inverting the indole ring and maximizing the overlap between the two six-membered rings. The atomic coordinates of the structures are provided in the Supporting Information. The model π stacks have quite different HT parameters and, therefore, represent distinct situations that can be encountered in natural and artificial systems. Note that the arrangement of G and Ind in π6 is similar to that found in the crystal structure of a complex of double-stranded RNA with the p19 protein (Protein Data Bank 1R9F).[31]

Calculation of Electron-Transfer Parameters. The HT rate (k_{HT}) between a pair of donor and acceptor states at each conformation is given by the Marcus equation[32]

$$k_{HT} = \frac{2\pi}{\hbar} V_{DA}^{\ 2} \frac{1}{\sqrt{4\pi\lambda k_B T}} \exp[-(\Delta G + \lambda)^2/4\lambda k_B T] \quad (1)$$

where ΔG is the driving force, V_{DA} is the electronic coupling between donor and acceptor, and λ is the reorganization energy. ΔG and V_{DA} can be obtained from the ab initio energies of the adiabatic states using the GMH method.[20] In this approach, one uses a unitary transformation U from the adiabatic to diabatic states. The diabatic Hamiltonian $\mathbf{H}$ is expressed through the diagonal matrix $\mathbf{E}$ of the adiabatic energy

$$\mathbf{U}^T\mathbf{E}\mathbf{U} = \mathbf{H} \quad (2)$$

In the two-state model, the off-diagonal element of $\mathbf{H}$ is the coupling V_{DA}, and the diagonal elements correspond to the site energies of the donor and acceptor.

dx.doi.org/10.1021/jp303675h | J. Phys. Chem. B 2012, 116, 7815−7820

Table 1. MS-CASPT2 Relative Energies (in eV), Dipole Moments (in au), and Transition Dipole Moments (in au) for $(G-Ind)^{\bullet+}$ π-Stacked Structures

	ΔE_{12}	ΔE_{13}	$\Delta\mu_{1,2}$[a]	$\Delta\mu_{1,3}$[a]	μ_{12}	μ_{13}	μ_{23}
π1	0.115	0.742	0.542	0.910	−2.272	−2.026	−1.786
π2	0.423	0.688	−0.567	−2.254	1.750	−2.459	2.554
π3	0.207	0.463	1.086	2.211	−2.984	1.827	1.303
π4	0.340	0.530	−4.124	2.194	3.047	0.026	0.186
π5	0.449	0.528	−2.24	1.861	−3.288	0.284	0.364
π6	0.043	0.271	3.182	4.600	−2.964	−1.027	−0.576

[a] $\Delta\mu_{i,j}$ = difference between the dipole moments of states j and $i = \mu_j - \mu_i$.

The transformation U of the adiabatic to diabatic states implies that the transition dipole moments between diabatic states should be zero, that is, the diabatic dipole moment matrix $\mathbf{M}_d$ should be diagonal. Therefore, $\mathbf{U}$ is the unitary matrix that diagonalizes the adiabatic dipole moment matrix $\mathbf{M}_{ad}$

$$\mathbf{U}^T\mathbf{M}_{ad}\mathbf{U} = \mathbf{M}_d \tag{3}$$

The diagonal elements of $\mathbf{M}_{ad}$ correspond to the dipole moments of the adiabatic states, and the off-diagonal elements correspond to the transition dipole moments. All elements of $\mathbf{M}_{ad}$ are obtained as projections of the ab initio dipole moments along the charge-transfer vector, defined as the vector connecting the centers of mass of the two molecules. The results obtained by projecting the dipole moments along the normal vector to the plane of the molecules were very similar (see Table SI2, Supporting Information).

In the two-state approach, V_{DA} can be obtained with the well-known formula[20]

$$|V_{DA}^{2\text{-st}}| = \frac{(E_2 - E_1)|\mu_{12}|}{[(\mu_1 - \mu_2)^2 + 4\mu_{12}{}^2]^{1/2}} \tag{4}$$

where μ_i is the projection of the dipole moment of state i along the charge-transfer vector and μ_{12} is the projection of the transition dipole moment. Then, the diabatic gap $\Delta\varepsilon = \varepsilon_D - \varepsilon_A$ is given by

$$\Delta\varepsilon = \sqrt{(E_2 - E_1)^2 - 4V_{DA}{}^2} \tag{5}$$

In addition to the ground states of G^+ and Ind^+, $Ind_1{}^+$, the three-state model includes the first excited state of the Ind^+ radical cation, $Ind_2{}^+$. In this case, the matrix $\mathbf{H}$ (eq 2) must be block diagonalized to set the couplings between the $Ind_1{}^+$ and $Ind_2{}^+$ states to zero.[20] The coupling elements and the diabatic energies are obtained after this transformation, and the resulting quasidiabatic matrix has the form shown

$$\mathbf{H}_{qd} = \begin{pmatrix} \varepsilon_{Ind_1{}^+} & V_{GS\text{-}CT} & 0 \\ V_{GS\text{-}CT} & \varepsilon_{G^+} & V_{ES\text{-}CT} \\ 0 & V_{ES\text{-}CT} & \varepsilon_{Ind_2{}^+} \end{pmatrix} \tag{6}$$

where the coupling between the G^+ and $Ind_1{}^+$ states is labeled with the subscript GS-CT and that between the G^+ and $Ind_2{}^+$ states is labeled ES-CT.

RESULTS AND DISCUSSION

The results of the ab initio calculations (MS-CASPT2 relative energies and dipole moment matrix elements from the PM-CASCI wave function) are summarized in Table 1. Using the ab initio values, we calculated the couplings and free energy differences for the six conformers with the two-state and three-state GMH treatments. In this section, we begin discussing a criterion, based on the dipole moments of the diabatic states, to anticipate whether the two-state approximation is sufficiently accurate or three states should be included in the GMH scheme. We then discuss the differences in the parameters obtained with the two approaches and consider an effective two-state treatment that accounts for the effect of the excited state $Ind_2{}^+$.

Suitability of the Two-State and Three-State Treatments. The GMH approach relies on the fact that the transformation defined by eq 3 yields proper diabatic states, which implies that, for each diabatic state, the extra charge must be well localized on the donor or the acceptor. This condition can be assessed examining the difference between the dipole moments of the diabatic states (diagonal elements of $\mathbf{M}_d$) and comparing it with the change in dipole moment estimated using the point-charge model for a perfect electron transfer, $\Delta\mu_{id} = er_{DA}$,[20] where e is the electron charge. For each conformation, r_{DA} is approximated as the distance between the centers of mass of G and Ind.

One important issue for the two-state treatment is how to pick the two adiabatic states, which should correspond to linear combinations of diabatic states G^+ and $Ind_1{}^+$. The obvious choice—the two lowest adiabatic states, D_0 and D_1—is not always correct. In our calculations, the guanine ring was found to lie in the xy plane, with the indole ring lying parallel to the plane, at positive values of z. Therefore, the adiabatic counterpart of the G^+ state (the state with highest positive charge on the guanine ring) can be identified as the state with the lowest relative dipole moment (see Table 1). In the π2 conformation, this is the D_2 state, so we applied the two-state GMH treatment to D_0 and D_2. In the remaining cases, we considered the D_0 and D_1 states.

The dipole moment differences obtained after the two-state and three-state treatments ($\Delta\mu_d^{2\text{-st}}$ and $\Delta\mu_d^{3\text{-st}}$, respectively) for each conformation are listed in Table 2, together with the values of $\Delta\mu_{id}$. The three-state GMH approach provides one G localized diabatic state (G^+) and two Ind localized ones ($Ind_1{}^+$ and $Ind_2{}^+$). For conformations π1−π3, there are substantial differences between $\Delta\mu_d^{2\text{-st}}$ and the ideal values (Table 2). These deviations are corrected by inclusion of the third state in the transformation. For conformations π4−π6, the two-state scheme already gives the proper diabatic states, and the $\Delta\mu_d^{2\text{-st}}$ values reproduce the ideal values well. Table 2 also shows that the three-state GMH approach provides a good description of the electron transfer in all cases, because the dipole moment differences between the G^+ state and the $Ind_1{}^+$ and $Ind_2{}^+$ states are in good agreement with the ideal values. Small deviations were obtained (within 10% in almost all cases) and are probably due to the way the charge-transfer vector is defined in $\Delta\mu_{id}$. This vector is defined as the vector between the center of

dx.doi.org/10.1021/jp303675h | J. Phys. Chem. B 2012, 116, 7815−7820

Table 2. Dipole Moment Differences (in au) of Donor and Acceptor Diabatic States Obtained Using the Two-State and Three-State GMH Treatments ($\Delta\mu_d^{2\text{-st}}$ and $\Delta\mu_d^{3\text{-st}}$, respectively), Ideal Changes in the Dipole Moments ($\Delta\mu_{id}$), and Parameter λ_D Calculated with Eq 7

structure	$\Delta\mu_d^{2\text{-st}}$	$\Delta\mu_{CT\text{-}GS}^{3\text{-st}}$	$\Delta\mu_{CT\text{-}ES}^{3\text{-st}}$	$\Delta\mu_{id}$	λ_D
$\pi1$	4.58	6.19	6.14	6.56	1.751
$\pi2$	5.41[a]	7.30	6.98	7.75	1.078
$\pi3$	6.07	7.01	6.44	7.71	0.361
$\pi4$	7.36	7.34	7.96	7.81	0.000
$\pi5$	6.95	6.98	6.52	6.84	0.008
$\pi6$	6.73	6.95	6.79	6.94	0.043

[a]Obtained after applying the two-state model to the D_0 and D_2 adiabatic states.

mass of the two molecules, but it does not consider the charge distribution in the two molecules. On the other hand, the energy difference between the third and fourth adiabatic states was found to be larger than 1 eV in all cases, which indicates that it is not necessary to include further states in the GMH treatment.

Our analysis can be compared with the diagnostic developed by Cave and co-workers.[21] This diagnostic, based on applying Löwdin partitioning theory to the adiabatic dipole moment matrix **M**, suggests that the two-state treatment is adequate when

$$\lambda_D = \left| \frac{\mu_{13}\mu_{32}}{\mu_{12}(\mu_2 - \mu_3)} \right| \ll 1 \tag{7}$$

Otherwise, a third state must be included in the calculation of electronic coupling. The diagnostic indicates that the three-state model must be applied to cases 1 and 2, whereas smaller effects can be expected for case 3. This prediction is similar to that derived by our comparison of diabatic dipole moments.

Calculated Parameters. The coupling elements and the diabatic gaps $\Delta\varepsilon$ derived with the two- and three-state GMH treatments for the six conformations of interest are reported in Table 3. The superscripts indicate which treatment was used to derive the parameters. The parameters for HT between G^+ and the ground state, Ind_1^+, are labeled with the subscript GS-CT. We also include the parameters for HT from the G^+ state to the indole excited state, Ind_2^+, labeled ES-CT. Finally, we include the free energy difference for an effective two-state treatment, as explained below.

We begin our analysis comparing the hole-transfer parameters between the G^+ and Ind_1^+ states ($V_{GS\text{-}CT}$ and $\Delta\varepsilon_{GS\text{-}CT}$) obtained with the two- and three-state treatments. The diabatic dipole moments discussed in the previous section (Table 2) suggest that the two-state treatment should provide reasonable values for conformations $\pi4-\pi6$. The calculated quantities (Table 3) are in line with this prediction, and there is almost perfect agreement between the data derived with the two- and three-state GMH schemes. Therefore, we focus our analysis on cases $\pi1-\pi3$. For conformation $\pi3$, there is reasonable agreement between the coupling values. However, the free energy differs significantly, as $\Delta\varepsilon_{GS\text{-}CT}^{3\text{-st}}$ is 0.05 eV lower than $\Delta\varepsilon_{GS\text{-}CT}^{2\text{-st}}$. Conformation $\pi1$ corresponds to the first case described by Cave and co-workers,[21] where the three adiabatic states are strong mixtures of the diabatic states. This can be recognized from Table 1, which shows small dipole moment differences between the adiabatic states. In agreement with this, the values of $\Delta\varepsilon_{GS\text{-}CT}^{3\text{-st}}$ and $\Delta\varepsilon_{GS\text{-}CT}^{2\text{-st}}$ differ by almost 0.2 eV. Conformation $\pi2$ deserves a more detailed comment. It corresponds to the second case,[21] where the G^+ state is close to the Ind_2^+ state and both states are well-separated from the Ind_1^+ state. Because of the strong mixing between the G^+ and Ind_2^+ states, the adiabatic counterpart of the G^+ state is the D_2 state (see our discussion above). Therefore, the two-state treatment was carried out for the D_0 and D_2 states. Comparison of the two- and three-state parameters shows substantial differences, in particular for the coupling, which differs by almost 0.1 eV. The parameters for $\pi2$ obtained with the two-state treatment of D_0 and D_1 are also listed in Table 3. Because this pair of states does not properly describe the HT, $\Delta\varepsilon_{GS\text{-}CT}^{2\text{-st}}$ and $\Delta\varepsilon_{GS\text{-}CT}^{3\text{-st}}$ differ significantly, by almost 0.3 eV. The $\Delta\varepsilon$ values found for distinct conformations can differ by 0.2–0.3 eV, which suggests significant effects of structural fluctuations on the driving force of HT. We expect that the variation of the redox potentials of the donor and acceptor species should be of the same magnitude (~0.4 eV) as found for HT in DNA.[33,34]

In Table 3, we also include the parameters for hole transfer between the G^+ and Ind_2^+ states. In principle, HT between these two states could contribute to the overall hole-transfer rate from guanine to indole. In some cases (conformations $\pi1-\pi3$), the couplings are quite strong, but the HT is always endothermic. Therefore, HT to the Ind_1^+ state is more favored thermodynamically, and the contribution of HT between the G^+ and Ind_2^+ states is negligible.

For practical reasons, taking into account the fact that HT to the Ind_2^+ state can be neglected, it is convenient to describe HT with an effective two-state Hamiltonian. Such an effective Hamiltonian can be derived by applying the Löwdin partitioning method to the quasidiabatic three-state Hamiltonian (eq 6). It has the form

$$\mathbf{H}^{\text{eff}}(E) = \mathbf{H}^0 - \begin{pmatrix} 0 \\ V_{ES\text{-}CT} \end{pmatrix} \frac{1}{E - \varepsilon_{Ind_2^+}} (0 \quad V_{ES\text{-}CT}) \tag{8}$$

Table 3. Coupling Elements (V) and Diabatic Energy Differences ($\Delta\varepsilon$) Derived with the Two- And Three-State GMH Treatments for the Six Conformations $\pi1-\pi6$[a]

structure	$V_{GS\text{-}CT}^{2\text{-st}}$	$\Delta\varepsilon_{GS\text{-}CT}^{2\text{-st}}$	$V_{GS\text{-}CT}^{3\text{-st}}$	$\Delta\varepsilon_{GS\text{-}CT}^{3\text{-st}}$	$V_{ES\text{-}CT}^{3\text{-st}}$	$\Delta\varepsilon_{ES\text{-}CT}^{3\text{-st}}$	$\Delta\varepsilon_{GS\text{-}CT}^{\text{eff}}$
$\pi1$	0.057	0.014	0.067	−0.169	0.301	0.331	0.010
$\pi2$[b]	0.313 (0.209)	−0.287 (−0.068)	0.228	−0.345	0.147	0.056	−0.224 (−0.276)
$\pi3$	0.102	0.037	0.110	−0.016	0.118	0.280	0.028
$\pi4$	0.141	−0.190	0.141	−0.191	0.004	0.265	−0.191
$\pi5$	0.212	−0.145	0.212	−0.146	0.008	0.230	−0.146
$\pi6$	0.019	0.020	0.019	0.012	0.045	0.244	0.020

[a]Energies in eV. [b]Two-state parameters and effective free energy calculated using the D_0 and D_2 adiabatic states. Data obtained from the D_0 and D_1 states shown in brackets.

where $\mathbf{H}^0$ is the upper (2 × 2) block of $\mathbf{H}_{qd}$. Equation 8 suggests that the effective coupling, $V^{eff}_{GS\text{-}CT}$, is equal to the three-state coupling, $V^{3\text{-}st}_{GS\text{-}CT}$, and the effective two-state free energy is given by

$$\Delta\varepsilon^{eff}_{GS\text{-}CT} = \Delta\varepsilon^{3\text{-}st}_{GS\text{-}CT} - \frac{V_{ES\text{-}CT}{}^2}{E - \varepsilon_{Ind_2{}^+}} \quad (9)$$

To calculate $\Delta\varepsilon^{eff}_{GS\text{-}CT}$, the parameter E was taken as the average of the D_0 and D_1 adiabatic energies, except for $\pi 2$, for which we used the energies of D_0 and D_2. For the latter case, the effective value was also obtained by treating D_0 and D_1 (in parentheses). The derived $\Delta\varepsilon^{eff}_{GS\text{-}CT}$ values are listed in the last column of Table 3. As can be seen, the ET parameters obtained within the two-state GMH scheme can deviate significantly from the corresponding matrix elements of the two-state effective Hamiltonian based on the GMH treatment of three adiabatic states.

The effect of the excited state, $Ind_2{}^+$, on the HT parameters is mainly caused by the small energy gap between this state and the ground state of the indole radical cation. The calculation was done in the gas phase. We do not expect, however, that accounting for polar surroundings could significantly change this gap because the hole remains localized on the relatively small indole fragment in both electronic states. Therefore, the first excited state of the tryptophan radical cation could have a marked impact on HT in biological systems.

CONCLUSIONS

Hole transfer (HT) from nucleobases to amino acid residues in DNA−protein complexes can play an important role in preventing oxidative damage of DNA in living cells. In this work, we have performed MS-CASPT2 calculations of several model structures of π-stacked guanine and indole and derived HT parameters for these systems using the generalized Mulliken−Hush method.

We found that the two-state model commonly applied to treat thermal ET between adjacent donor and acceptor can be of limited use when HT between guanine and indole is treated. The HT parameters obtained within the two-state scheme can deviate considerably from the corresponding values derived with the three-state model. Therefore, to guarantee a proper description of the system, three adiabatic states must be included in the GMH transformation. This is required because of the small gap between the ground and first excited states in the indole radical cation. In this respect, HT in the $(G-Ind)^{\bullet+}$ system is substantially different from that in DNA, where the ground and excited states of radical cations are well-separated and, consequently, the two-state model can be employed. We found that comparison of a two-state diabatic dipole moment with the value derived using the simple point-charge model provides a convenient test to identify situations where the two-state scheme can fail. We demonstrated that the diabatic energy gap for HT found with the three-state approach should be modified according to eq 9 to properly describe the HT between G and Ind and in other systems with close-lying excited states. In the effective two-state model, the donor−acceptor coupling is equal to the value provided by the three-state approach.

The obtained electron-transfer parameters can be used as benchmarks to assess the accuracy of less sophisticated approaches that have lower computational costs. For example, these benchmarks can be employed to evaluate DFT methods, which have already been applied to explore hole transfer in biological models.[23−27]

ASSOCIATED CONTENT

Supporting Information

MS-CASPT2 energies (Table SI1), HT parameters obtained using the dipole moment projection along the normal vector to the plane of the molecules (Table SI2), comparison of HT parameters derived from CASPT2 and CASSCF calculations (Tables SI3), and Cartesian coordinates of all structures. This material is available free of charge via the Internet at http://pubs.acs.org.

AUTHOR INFORMATION

Corresponding Author

*E-mail: lluis.blancafort@udg.edu (L.B.), alexander.voityuk@icrea.cat (A.V.).

Notes

The authors declare no competing financial interest.

ACKNOWLEDGMENTS

Financial support from MICINN (Ministry of Science and Innovation, Spain) and the FEDER fund (European Fund for Regional Development) was provided by Grants CTQ 2011-26573, CTQ 2011-23441 and UNGI08-4E-003, UNGI10-4E-801, respectively. Financial support from the Generalitat de Catalunya (SGR528 and Xarxa de Referència en Química Teòrica i Computacional) is also acknowledged.

REFERENCES

(1) Genereux, C. G.; Barton, J. K. *Chem. Rev.* **2010**, *110*, 1642−1662.
(2) Schuster, G. B., Ed. *Long-Range Charge Transfer in DNA*; Topics in Current Chemistry Series; Springer: Berlin, 2004; Vol. *236*.
(3) Berlin, Y. A.; Kurnikov, I. V.; Beratan, D.; Ratner, M. A.; Burin, A. L. *Top. Curr. Chem.* **2004**, *237*, 1−36.
(4) Venkatramani, R.; Keinan, S.; Balaeff, A.; Beratan, D. N. *Coord. Chem. Rev.* **2011**, *255*, 635−648.
(5) Siriwong, K.; Voityuk, A. A. *WIREs Comput. Mol. Sci.*, published online Mar 29, 2012, 10.1002/wcms.1102.
(6) Genereux, J. C.; Boal, A. K.; Barton, J. K. *J. Am. Chem. Soc.* **2010**, *132*, 891−905.
(7) Sancar, A. *Chem. Rev.* **2003**, *103*, 2203−2237.
(8) Prytkova, T. R.; Beratan, D. N.; Skourtis, S. S. *Proc. Natl. Acad. Sci. U.S.A.* **2007**, *104*, 802−807.
(9) Woiczikowski, P. B.; Steinbrecher, T.; Kubař, T.; Elstner, M. *J. Phys. Chem. B* **2011**, *115*, 9846−9863.
(10) Milligan, J. R.; Tran, N. Q.; Ly, A.; Ward, J. F. *Biochemistry* **2004**, *43*, 5102−5108.
(11) Wagenknecht, H. A.; Stemp, E. D. A.; Barton, J. K. *J. Am. Chem. Soc.* **2000**, *122*, 1−7.
(12) Wagenknecht, H. A.; Rajski, S. R.; Pascaly, M.; Stemp, E. D. A.; Barton, J. K. *J. Am. Chem. Soc.* **2001**, *123*, 4400−4407.
(13) Jena, N. R.; Mishra, P. C.; Suhai, S. *J. Phys. Chem. B* **2009**, *113*, 5633−5644.
(14) Dumont, A.; Zheng, Y.; Hunting, D.; Sanche, L. *J. Chem. Phys.* **2010**, *132*, 045102.
(15) Butchosa, C.; Simon, S.; Voityuk, A. A. *Org. Biomol. Chem.* **2010**, *8*, 1870−1875.
(16) Butchosa, C.; Simon, S.; Voityuk, A. A. *Int. J. Quantum Chem.* **2012**, *112*, 1838−1843.
(17) Butchosa, C.; Simon, S.; Voityuk, A. A. *Comput. Theor. Chem.* **2011**, *975*, 38−41.
(18) Robinson, J. W. *Handbook of Spectroscopy*; CRC Press: Boca Raton, FL, 1980; Vol. *1*.

(19) Roca-Sanjuán, D; Rubio, M; Merchán, M; Serrano-Andrés, L. *J. Chem. Phys.* **2006**, *125*, 084302.
(20) Cave, R. J.; Newton, M. D. *J. Chem. Phys.* **1997**, *106*, 9213−9226.
(21) Rust, M.; Lappe, J.; Cave, R. J. *J. Phys. Chem. A* **2002**, *106*, 3930−3940.
(22) Blancafort, L.; Voityuk, A. A. *J. Phys. Chem. A* **2006**, *110*, 6426−6432.
(23) Kubař, T.; Woiczikowski, P. B.; Cuniberti, G.; Elstner, M. *J. Phys. Chem. B* **2008**, *112*, 7937−7947.
(24) Migliore, A.; Corni, S.; Varsano, D.; Klein, M. L.; Di Felice, R. *J. Phys. Chem. B* **2009**, *113*, 9402−9415.
(25) Felix, M.; Voityuk, A. A. *Int. J. Quantum Chem.* **2011**, *111*, 191−201.
(26) Felix, M.; Voityuk, A. A. *J. Phys. Chem. A* **2008**, *112*, 9043−9049.
(27) Voityuk, A. A. *Chem. Phys. Lett.* **2006**, *427*, 177−180.
(28) Finley, J.; Malmqvist, P. A.; Roos, B. O.; Serrano-Andres, L. *Chem. Phys. Lett.* **1998**, *288*, 299−306.
(29) Roos, B. O.; Andersson, K. *Chem. Phys. Lett.* **1995**, *245*, 215−223.
(30) Aquilante, F.; De Vico, L.; Ferre, N.; Ghigo, G.; Malmqvist, P.-A.; Neogrady, P.; Pedersen, T. B.; Pitonak, M.; Reiher, M.; Roos, B. O.; Serrano-Andrés, L.; Urban, M.; Veryazov, V.; Lindh, R. *J. Comput. Chem.* **2010**, *31*, 224−247.
(31) Ye, K.; Malinina, L.; Patel, D. J. *Nature* **2003**, *426*, 874.
(32) Marcus, R. A.; Sutin, N. *Biochim. Biophys. Acta* **1985**, *811*, 265−322.
(33) Voityuk, A. A.; Siriwong, K.; Rösch, N. *Angew. Chem., Int. Ed.* **2004**, *43*, 624−627.
(34) Kubař, T.; Kleinekathofer, U.; Elstner, M. *J. Phys. Chem. B* **2009**, *113*, 13107.